



# 1 Dynamics of deep soil carbon – insights from $^{14}\text{C}$ time-series 2 across a climatic gradient

3  
4 Tessa Sophia van der Voort<sup>1</sup>, Utsav Mannu<sup>1,†</sup>, Frank Hagedorn<sup>2</sup>, Cameron McIntyre<sup>1,3</sup>,

5 Lorenz Walthert<sup>2</sup>, Patrick Schlegel<sup>2</sup>, Negar Haghpor<sup>1</sup>, Timothy Ian Eglinton<sup>1</sup>

6 <sup>1</sup>Institute of Geology, ETH Zürich, Sonneggstrasse 5, 8092 Zürich, Switzerland

7 <sup>2</sup>Forest soils and Biogeochemistry, Swiss Federal Research Institute WSL, Zürcherstrasse 111, 8903  
8 Birmensdorf, Switzerland

9 <sup>3</sup>Department of Physics, Laboratory of Ion Beam Physics, ETH Zurich, Schaffmattstrasse 20, 9083 Zurich

10 <sup>†</sup>New address: Department of Earth and Climate Science, IISER Pune, Pune, India

11

12 *correspondence to:* Tessa Sophia van der Voort ([tessa.vandervoort@erdw.ethz.ch](mailto:tessa.vandervoort@erdw.ethz.ch))

13

14 **Abstract.** Quantitative constraints on soil organic matter (SOM) dynamics are essential for comprehensive  
15 understanding of the terrestrial carbon cycle. Deep soil carbon is of particular interest, as it represents large  
16 stocks and its turnover rates remain highly uncertain. In this study, SOM dynamics in both the top and deep soil  
17 across a climatic (average temperature  $\sim 1\text{--}9\text{ }^{\circ}\text{C}$ ) gradient are determined using time-series ( $\sim 20$  years)  $^{14}\text{C}$  data  
18 from bulk soil and water-extractable organic carbon (WEOC). Analytical measurements reveal enrichment of  
19 bomb-derived radiocarbon in the deep soil layers on the bulk level during the last two decades. The WEOC pool  
20 is strongly enriched in bomb-derived carbon, indicating that it is a dynamic pool. A numerical model was  
21 constructed to determine turnover time of the bulk, slow and dynamic pool as well as the size of the dynamic  
22 pool. The presence of bomb-derived carbon in the deep soil, as well as the rapidly turning over WEOC pool and  
23 sizeable dynamic fraction at depth across the climatic gradient implies that there likely is a dynamic component  
24 of carbon in the deep soil. Precipitation and bedrock type appear to exert a stronger influence on soil C turnover  
25 and stocks as compared to temperature.

26

## 27 1 Introduction

28 Within the broad societal challenges accompanying climate and land use change, a better understanding of the  
29 drivers of turnover of carbon in the largest terrestrial reservoir of organic carbon, as constituted by soil organic  
30 matter (SOM), is essential (Batjes, 1996; Davidson and Janssens, 2006; Doetterl et al., 2015; Prietzel et al.,  
31 2016). Terrestrial carbon turnover remains one of the largest uncertainties in climate model predictions  
32 (Carvalhais et al., 2014; He et al., 2016). At present, there is no consensus on the net effect that climate and land  
33 use change will have on SOM stocks (Crowther et al., 2016; Gosheva et al., 2017; Melillo et al., 2002; Schimel  
34 et al., 2001; Trumbore and Czimczik, 2008). Deep soil carbon is of particular interest because of its large stocks  
35 (Jobbagy and Jackson, 2000; Rumpel and Kogel-Knabner, 2011) and perceived stability. The stability is  
36 indicated by low  $^{14}\text{C}$  content (Rethemeyer et al., 2005; Schrumpp et al., 2013; van der Voort et al., 2016) and  
37 low microbial activity (Fierer et al., 2003). Despite its importance, deep soil carbon has been sparsely studied  
38 and remains poorly understood (Angst et al., 2016; Rumpel and Kogel-Knabner, 2011). The inherent complexity  
39 of SOM and the multitude of drivers controlling its stability further impedes the understanding of this globally  
40 significant carbon pool (Schmidt et al., 2011). In this framework, there is a particular interest in the portion of  
41 soil carbon that could be most vulnerable to change, especially in colder climates (Crowther et al., 2016).



42 Water-extractable organic carbon (WEOC) is seen as a dynamic and potentially vulnerable carbon pool in the soil  
43 (Hagedorn et al., 2004; Lechleitner et al., 2016). Radiocarbon ( $^{14}\text{C}$ ) can be a powerful tool to determine the  
44 dynamics of carbon turnover over decadal to millennial timescales because of the incorporation of bomb-  
45 derived  $^{14}\text{C}$  introduced in the atmosphere in the 1950's as well as the radioactive decay of  $^{14}\text{C}$  naturally present  
46 in the atmosphere (Torn et al., 2009). Time-series  $^{14}\text{C}$  data is particularly insightful because it enables the  
47 tracking of recent decadal carbon. Furthermore, single time-point  $^{14}\text{C}$  data can yield two estimates for turnover  
48 time, whilst time-series data yields a single turnover estimate (Torn et al., 2009). Given that the so-called “bomb  
49 radiocarbon spike” will continue to diminish in the coming decades, time-series measurements are increasingly  
50 a matter of urgency in order to take full advantage of this intrinsic tracer (Graven, 2015). Several case-studies  
51 have collected time-series  $^{14}\text{C}$  soil datasets and demonstrated the value of this approach (Baisden and Parfitt,  
52 2007; Prior et al., 2007; Fröberg et al., 2010; Mills et al., 2013, Schrumpf and Kaiser, 2015). However, these  
53 studies are sparse, based on specific single sites and have been rarely linked to abiotic and biotic parameters.  
54 Much more is yet to be learned about the carbon cycling through time-series observations in top- and subsoils  
55 along environmental gradients. Furthermore, to our knowledge, there are no studies with pool-specific  $^{14}\text{C}$  soil  
56 time-series focusing on labile carbon.

57

58 This study assesses two-pool soil carbon dynamics as determined by time-series (~20 years) radiocarbon across  
59 a climatic gradient. The time-series data is analyzed by a numerically optimized model with a robust error  
60 reduction to yield carbon turnover estimates for the bulk, dynamic and slow pool. Model output is linked to  
61 potential drivers such as climate, forest productivity and physico-chemical soil properties. The overall objective  
62 of this study is to improve our understanding of shallow and deep soil carbon dynamics in a wide range of  
63 ecosystems.

64

## 65 **2 Materials and methods**

### 66 **2.1 Study sites, sampling strategy and WEOC extraction**

67 The five sites investigated in this study are located in Switzerland between 46–47° N and 6–10° E and  
68 encompass large climatic (mean annual temperature (MAT) 1.3–9.2°C, mean annual precipitation (MAP) 864–  
69 2126 mm  $\text{m}^{-2}\text{y}^{-1}$ ) and geological gradients (Table 1). The sites are part of the Long-term Forest Ecosystem  
70 Research program (LWF) at the Swiss Federal Institute for Forest, Snow and Landscape Research, WSL  
71 (Schaub et al., 2011; Etzold et al., 2014). The soils of these sites were sampled between 1995 and 1998  
72 (Walthert et al., 2002, 2003) and were re-sampled following the same sampling strategy in 2014 with the aim to  
73 minimize noise caused by small-scale soil heterogeneity. In both instances sixteen samples were taken on a  
74 regular grid on the identical 43 by 43 meters (~1600  $\text{m}^2$ ) plot (Fig. 1; see Van der Voort et al., 2016 for further  
75 details). For the archived samples taken between 1995 and 1998, mineral soil samples down to 40 cm depth  
76 (intervals of 0–5, 5–10, 10–20 and 20–40 cm) were taken on an area of 0.5 by 0.5 m (0.25  $\text{m}^2$ ). For samples >40  
77 cm (intervals of 40–60, 60–80 and 80–100 cm), corers were used to acquire samples ( $n=5$  in every pit, area  
78 ~2.8×10<sup>-3</sup>  $\text{m}^2$ ). The organic layer was sampled by use of a metal frame (30×30 cm). The samples were dried at  
79 35–40°C, sieved to remove coarse material (2 mm), and stored in hard plastic containers under controlled  
80 climate conditions in the “Pedothek” at WSL (Walthert et al., 2002). For the samples acquired in 2014 the same  
81 sampling strategy was followed, and samples were taken on the exact same plot proximal (~10 m) to the legacy



82 samples. For the sampling, a SHK Martin Burch AG HUMAX soil corer ( $\sim 2 \times 10^3 \text{ m}^2$ ) was used for all depths  
83 (0–100 cm). For the organic layer, a metal frame of 20×20 cm was used to sample. Samples were sieved (2 mm),  
84 frozen and freeze-dried using an oil-free vacuum-pump powered freeze dryer (Christ, Alpha 1-4 LO *plus*). For  
85 the time-series radiocarbon measurements, all samples covering  $\sim 1600 \text{ m}^2$  were pooled to one composite sample  
86 per soil depth using the bulk-density. In order to determine bulk-density of the fine earth of the 2014 samples,  
87 stones > 2 mm were assumed to have a density of  $2.65 \text{ g/cm}^3$ . For the Alptal site, sixteen cores were taken on a  
88 slightly smaller area ( $\sim 1500 \text{ m}^2$ ) which encompasses the control plot of a nitrogen addition experiment  
89 (NITREX project) (Schleppi et al., 1998). For this site, no archived samples are available and thus only the 2014  
90 samples were analyzed. Soil carbon stocks were estimated by multiplying SOC concentrations with the mass of  
91 soil calculated from measured bulk densities and stone contents for each depth interval (Gosheva et al., 2017).  
92 For the Nationalpark site, the soil carbon stocks from 80–100 cm were estimated using data from a separately  
93 dug soil profile (Walthert et al., 2003) because the HUMAX corer could not penetrate the rock-dense soil below  
94 80 cm depth. In order to understand very deep soil carbon dynamics (i.e. >100 cm), this study also includes  
95 single-time point  $^{14}\text{C}$  analyses of soil profiles that were dug down to the bedrock between 1995 and 1998 as part  
96 of the LWF programme on the same sites (Walthert et al., 2002). The sampling of the profiles has not yet been  
97 repeated.

98

## 99 2.2 Climate and soil data

100 Temperature and precipitation data are derived from weather stations close to the study sites that have been  
101 measuring for over two decades, yielding representative estimates of both variables and over the time period  
102 concerned in this study (Etzold et al., 2014). The pH values for all sites and concerned depth intervals were  
103 acquired during the initial sampling campaign (Walthert et al. 2002). At Alptal, pH values were determined as  
104 described in Xu et al. (2009), values of 10–15 cm were extrapolated to the deeper horizons because of the  
105 uniform nature of the Gley horizon. Exchangeable cations were extracted (in triplicate) from the 2-mm-sieved  
106 soil in an unbuffered solution of 1 M  $\text{NH}_4\text{Cl}$  for 1 hour on an end-over-end shaker using a soil-to-extract ratio of  
107 1:10. The element concentrations in the extracts were determined by inductively coupled plasma atomic  
108 emission spectroscopy (ICP-AES) (Optima 3000, Perkin–Elmer). Contents of exchangeable protons were  
109 calculated as the difference between the total and the Al-induced exchangeable acidity as determined (in  
110 duplicate) by the KCl method (Thomas, 1982). This method was applied only to soil samples with a pH ( $\text{CaCl}_2$ )  
111 < 6.5. In samples with a higher pH, we assumed the quantities of exchangeable protons were negligible. The  
112 effective cation-exchange capacity (CEC) was calculated by summing up the charge equivalents of  
113 exchangeable Na, K, Mg, Ca, Mn, Al, Fe and H. The base saturation (BS) was defined as the percental fraction  
114 of exchangeable Na, K, Mg, and Ca of the CEC (Walthert et al., 2002, 2013). Net primary production (NPP)  
115 was determined by Etzold et al. (2014) as the sum of carbon fluxes by woody tree growth, foliage, fruit  
116 production and fine root production. Soil texture (sand, silt and clay content) on plot-averaged samples taken in  
117 2014 have been determined using grain size classes for sand, silt and clay respectively of 0.05–2 mm, 0.002–0.05  
118 mm and <0.002 mm according to Klute (1986). The continuous distribution of grain sizes was also determined  
119 after removal of organic matter (350 °C for 12 h) using the Mastersizer 2000 (Malvern Instruments Ltd.). Soil  
120 water potential (SWP) was measured on the same sites as described in Von Arx et al., (2013).

121



122 **2.3 Isotopic ( $^{14}\text{C}$ ,  $^{13}\text{C}$ ) and compositional (C, N) analysis**

123 Prior to the isotopic analyses, inorganic carbon in all samples was removed by vapour acidification for 72 hours  
 124 (12M HCl) in desiccators at 60 °C (Komada et al., 2008). After fumigation, the acid was neutralised by  
 125 substituting NaOH pellets for another 48 hours. All glassware used during sample preparation was cleaned and  
 126 combusted at 450°C for six hours prior to use. Water extractable organic carbon (WEOC) was procured by  
 127 extracting dried soil with 0.5 wt% pre-combusted NaCl in ultrapure Milli-Q (MQ) water in a 1:4 soil:water  
 128 mass ratio (adapted from Hagedorn et al., (2004), details in Lechleitner et al., (2016)).

129 In order to determine absolute organic carbon and nitrogen content as well as  $^{13}\text{C}$  values, an Elemental  
 130 Analyser-Isotope Ratio Mass Spectrometer system was used (EA-IRMS, Elementar, vario MICRO cube –  
 131 Isoprime, Vison). Atropine (Säntis) and an in-house standard peptone (Sigma) were used for the calibration of  
 132 the EA-IRMS for respectively carbon concentration, nitrogen concentration and C:N ratios and  $^{13}\text{C}$ . High  $^{13}\text{C}$   
 133 values were used to flag if all inorganic carbon had been removed by acidification.

134 For the  $^{14}\text{C}$  measurements of the bulk soil samples were first graphitised using an EA-AGE (elemental analyser-  
 135 automated graphitization equipment, Ionplus AG) system at the Laboratory of Ion Beam Physics at ETH Zürich  
 136 (Wacker et al., 2009). Graphite samples were measured on a MICADAS (MINitirised radioCARbon DAting  
 137 System, Ionplus AG) also at the Laboratory of Ion Beam Physics, ETH Zürich (Wacker et al., 2010). For three  
 138 samples (Alptal depth intervals 40-60, 60-80 and 80-100 cm) the  $^{14}\text{C}$  signature was directly measured as  $\text{CO}_2$   
 139 gas using the recently developed online elemental analyzer (EA) - stable isotope ratio mass spectrometers  
 140 (IRMS)–AMS system at ETH Zürich (McIntyre et al., 2016). Oxalic acid (NIST SRM 4990C) was used as the  
 141 normalising standard. Phthalic anhydride and in-house anthracite coal were used as blank. Two in-house soil  
 142 standards (Alptal soil 0-5 cm, Othmarsingen soil 0-5 cm) were used as secondary standards. For the WEOC,  
 143 samples were converted to  $\text{CO}_2$  by Wet Chemical Oxidation (WCO) (Lang et al., 2016) and run on the AMS  
 144 using a Gas Ion Source (GIS) interface (Ionplus). To correct for contamination, a range of modern standards  
 145 (sucrose, Sigma,  $\delta^{13}\text{C} = -12.4 \text{ ‰ VPDB}$ ,  $F^{14}\text{C} = 1.053 \pm 0.003$ ) and fossil standards (phthalic acid, Sigma,  
 146  $\delta^{13}\text{C} = -33.6 \text{ ‰ VPDB}$ ,  $F^{14}\text{C} < 0.0025$ ) were used (Lechleitner et al., 2016).

147

148 **2.4 Numerical optimization turnover and vulnerable fraction**

149 **2.4.1 Time-series based determination of likeliest turnover time**

150 In order to optimally constrain carbon turnover estimates for the  $^{14}\text{C}$  time-series data, a numerical model was  
 151 constructed in MATLAB version 2015a (The MathWorks, Inc., Natick, Massachusetts, United States). For the  
 152 turnover estimation, we assumed the system to be in steady state over the modeled period ( $\sim 1 \times 10^4$  years,  
 153 indicating soil formation since the last glacial retreat (Ivy-Ochs et al., 2009)), hence accounting both for  
 154 radioactive decay and incorporation of the bomb-testing derived material produced in the 1950's and 1960's  
 155 (Eq. 1.) (Herold et al., 2014; Torn et al., 2009).

156 
$$R_{\text{sample},t} = k \times R_{\text{atm},t} + (1 - k - \lambda) \times R_{\text{sample}(t-1)} \quad (1)$$

157 
$$R_{\text{sample},t} = \frac{\Delta^{14}\text{C}_{\text{sample}}}{1000} + 1 \quad (2)$$



158 In Eq. 1-2, the constant for radioactive decay of  $^{14}\text{C}$  is indicated as  $\lambda$ , the decomposition rate  $k$  (inverse of  
 159 turnover time) is the only unknown in this equation and is hence the variable for which the optimal value that  
 160 fits the data is sought using the model. The R value of the sample is inferred from  $\Delta^{14}\text{C}$ , hence accounting for  
 161 the sampling year, as shown in Eq. (2) (Herold et al., 2014; Solly et al., 2013). In order to avoid ambiguity the  
 162 term *turnover time* and not i.e. mean residence time is used solely in this manuscript (Sierra et al., 2016). For  
 163 computation of the optimal turnover time we assumed an initial fraction modern ( $F_m$ ) of  $^{14}\text{C}$  value of 1 at 10000  
 164 B.C.. For the period after 1900 atmospheric fraction modern ( $F_m$ ) values of the Northern Hemisphere were used  
 165 (Levin et al., 2010).

166 Using Eq. 1-2, we then computed the  $R_{\text{sample},t}$  for two given time points (1995-1998 A.D., depending on the  
 167 year of initial sampling and 2014 AD) within a range of turnover time of 1-10000 years. The exhaustive  
 168 numerical optimization evaluates the likelihood of every single solution (precision to 0.1 year) and yields the  
 169 turnover rate which is the optimal fit for the two data points (Fig. 2 and 3). In order to account for vegetation-  
 170 lag, two scenarios were run: firstly (1) with no assumed lag between the fixation of carbon from the atmosphere  
 171 and input into the soil and (2) model run with a lag of fixation of the atmospheric carbon as inferred from the  
 172 dominant vegetation (Von Arx et al., 2013; Etzold et al., 2014). In the case of full deciduous trees coverage a  
 173 lag of two years was assumed, and for the case of 100% conifer-dominated coverage a lag of 8 years was  
 174 incorporated (Table 1). Turnover times determined with the numerical optimization match the manually  
 175 optimized turnover modeling published previously (Herold et al., 2014; Solly et al., 2013).

#### 176 2.4.2 Turnover and size vulnerable pool based on two-pool model

177 As SOM is complex and composed of a continuum of pools with various ages (Schrumpf and Kaiser, 2015) and  
 178 there is data available from two SOM pools, a two-pool model was created (Fig. 3). WEOC constitutes only a  
 179 small portion of the total carbon (<1%), but could be representative for a larger component of rapidly turning  
 180 over carbon, even in the deep soil (Baisden and Parfitt, 2007; Koarashi et al., 2012). Using the data from the  
 181 bulk soil and WEOC time-series, the turnover of the slow pool and the relative size of the dynamic pool can be  
 182 determined. The following assumption were made: First, both pools (slow & fast) make up the total carbon pool  
 183 (Eq. 3). Secondly, the total turnover of the bulk soil is made up out of the “dynamic” fraction turnover  
 184 multiplied by “dynamic” fraction pool size and the “slow” pool turnover multiplied by “slow” pool size (Eq. 4).  
 185 Lastly, we assume that the signature of the sample (the time-series bulk data) is determined by the rate of  
 186 incorporation of the material (atmospheric signal) and the loss of carbon the two pools (Eq. 5).

$$187 \quad 1 = F_1 + F_2 \quad (3)$$

$$188 \quad k_{\text{total}} = (k_1 \cdot F_1) + (k_2 \cdot F_2) \quad (4)$$

$$189 \quad R_{\text{sample},t} = k_{\text{total}} \times R_{\text{atm},t} + F_1 [(1 - k_1 - \lambda) \times R_{\text{sample}(t-1)}] + F_2 (1 - k_2 - \lambda) \times R_{\text{sample}(t-1)} \quad (5)$$

190 Where  $F_1$  is the relative size of the dynamic pool, and  $F_2$  is the relative size of the (more) stable pool. The  $k_1$  is  
 191 the inverse of the turnover time of the WEOC as determined using the numerical optimisation of Eq. (1) and (2),  
 192 and  $k_2$  is determined by numerical optimisation. The  $k_2$  is the inverse of the turnover of the slow pool. The



193 numerical optimization finds the likeliest solution for the given dataset. Further details can be found in the  
194 Supplementary Information (SI) text and SI Fig. 1. Due to limited availability of archived samples, there are  
195 only single time points available for some samples as indicated in Fig. 4. The Matlab-based numerical  
196 optimization code will be made available upon publication. For correlations (packages HMISC, corrgram,  
197 method = pearson, significance  $p < 0.05$ ), statistical software R version 1.0.153 was used.

198

### 199 3 Results

#### 200 3.1 Changes of radiocarbon signatures over time

201 Overall, there is a pronounced decrease in radiocarbon signature with soil depth at all sites (Fig. 4). The time-  
202 series results show clear changes in radiocarbon signature over time from the initial sampling period (1995-  
203 1998) as compared to 2014, with the magnitude of change depending on site and soil depth. In the uppermost 5  
204 cm of soils, the overarching trend in the bulk soil is a decrease in the  $^{14}\text{C}$  bomb-spike signature in the warmer  
205 climates (Othmarsingen, Lausanne), whilst at higher elevation (colder) sites (Beatenberg, Nationalpark) the  
206 bomb-derived carbon appears to enter the top soil between 1995-8 and 2014.

207 Water-extractable OC (WEOC) has an atmospheric  $^{14}\text{C}$  signature in the top soil at all sites in 2014. The  
208 deep soil in the 1990's still has a negative  $\Delta^{14}\text{C}$  signature of WEOC at multiple sites. There are two  
209 distinguishable types of depth trends for WEOC in the 2014 dataset: (1) WEOC has the same approximate  $^{14}\text{C}$   
210 signature throughout depth (Othmarsingen, Beatenberg), (2) WEOC becomes increasingly  $^{14}\text{C}$  depleted with  
211 depth (Alptal, Nationalpark), or an intermediate form where WEOC  $^{14}\text{C}$  is modern throughout the top soil but  
212 becomes more depleted of  $^{14}\text{C}$  in the deep soil (Lausanne) (Fig. 4). The isotopic trends of WEOC co-vary with  
213 grain size as inherited from the bedrock type (Walthert et al., 2003). Soils with a relatively modern WEOC  
214 signature in 2014 (down to 40 cm) are underlain by bedrock with large grained (SI Fig. 3, Table SI 3)  
215 components (the moraines and sandstone at Othmarsingen, Lausanne and Beatenberg respectively). Soils where  
216 WEOC  $^{14}\text{C}$  signature decreases with depth are underlain by bedrock containing fine-grained components. For  
217 instance, the Flysch in Alptal (Schleppi et al., 1998) and intercalating layers of silt and coarse grained alluvial  
218 fan in Nationalpark (Walthert et al., 2003) respectively.

219

#### 220 3.2 Carbon turnover and the dynamic fraction

221 Incorporation of a vegetation-induced time lag (SI Fig. 2, Table 2) has an effect on modelled carbon dynamics  
222 in the organic layer, but this effect is strongly attenuated in the 0-5 cm layer in the mineral soil and virtually  
223 absent for the deeper soil layers. Turnover times show two modes of behavior for well-drained soils and  
224 hydromorphic soils, respectively. The non-hydromorphic soils have relatively similar values with decadal  
225 turnover times for the 0-5 cm layer, increasing to an order of centuries down to 20 cm depth, and to millenia in  
226 deeper soil layers (980 to 3940 years at 0.6 to 1 m depth) (Fig. 5). In contrast, the hydromorphic soils are  
227 marked by turnover times that are up to an order of magnitude larger, from centennial in top soil to (multi-)  
228 millennial in deeper soils. At the Beatenberg podsol, turnover time of the deepest layer (40-60 cm, ~1900 y) is  
229 faster than the shallow layer (20-40 cm, ~1300 y) (Figure 5, SI Table 5).

230 Carbon stocks also show distinct difference between drained and hydromorphic soils with greater stock in the  
231 hydromorphic soils (~15 kg C m<sup>-2</sup> at Beatenberg and Alptal vs. ~6 - ~7 kg C m<sup>-2</sup> at Othmarsingen, Lausanne  
232 and Nationalpark, Fig. 5, Table 3)).



233 The turnover times of the WEOC mimic the trends in the bulk soil but are up to an order of magnitude  
234 faster. Considering WEOC turnover in the non-hydromorphic soils only, there is a slight increase in WEOC  
235 turnover with decreasing site temperature, but the trend is not significant. The modeled dynamic fraction is  
236 sizeable at the surface but decreases towards the lower top soil (from ~0.4 at 0-5 cm to ~0.1 at 10-20 cm in  
237 Othmarsingen). In the deep soil, there is also a non-negligible proportion of dynamic carbon (e.g. 0.14-0.46 at  
238 20-40 cm).

239

### 240 3.3 Pre-glacial carbon in deep soil profiles

241 The turnover times of deep soil carbon exceed 10,000 years in several profiles, indicating the presence of carbon  
242 that pre-dates the glacial retreat (Fig. 6). These profiles are located on carbon-containing bedrock and concern  
243 the deeper soil (80-100 cm) of the Gleysol (Alptal), as well as >100 cm in the Cambisol (Lausanne) (Fig. 6).

244

### 245 3.4 Environmental drivers of carbon dynamics

246 Pearson correlation was used to assess potential relationships between carbon stocks, turnover and fluxes and  
247 their potential controlling factors (climate, NPP, soil texture, soil moisture and physicochemical properties  
248 (Table 4)). For the averaged top soil (0-20 cm, n=5), carbon stocks were significantly positive correlated to  
249 Mean Annual Precipitation (MAP). Turnover time in the bulk top soil negatively correlated with silt content and  
250 positively with average grain size. Turnover time in the WEOC of the top soil did not correlate significantly  
251 with any parameter. The modeled dynamic soil fraction in the top soil does positively correlate with MAP and  
252 clay content and negatively with sand content. Deeper soil bulk stock and turnover positively correlated with  
253 MAP and negatively with Cation Exchange Capacity (CEC). For non-hydromorphic sites, the fraction of  
254 dynamic carbon increases with decreasing MAT at all depths, but the trend is not significant (e.g. from ~0.4 -  
255 ~0.9 at 0-5 cm).

256

## 257 4 Discussion

### 258 4.1 Dynamic deep soil carbon

#### 259 4.1.1 Rapid shifts in $^{14}\text{C}$ abundance reflect dynamic deep carbon

260 The propagation of bomb-derived carbon into supposedly stable deep soil on the bulk level across the climatic  
261 gradient implies that SOM in deep soil contains a dynamic pool and could be less stable and potentially more  
262 vulnerable to change than previously thought. This possibility is further supported by the WEO $^{14}\text{C}$  which is  
263 consistently more enriched in bomb-derived carbon than the bulk soil. Near-atmospheric signature WEO $^{14}\text{C}$   
264 pervades up to 40 or even 60 cm depth. Hagedorn et al., (2004) also found WEOC to be a highly dynamic pool  
265 using  $^{13}\text{C}$  tracer experiments in forest soils.

266 We consider our  $^{14}\text{C}$  comparison over time to be robust because the grid-based sampling and averaging was  
267 repeated on the same plots which excludes the effect plot-scale variability (Van der Voort et al., 2016). Our  $^{14}\text{C}$   
268 time-series data in the deep soil corroborate pronounced changes in  $^{14}\text{C}$  (hence substantial SOM turnover) in  
269 subsoils of an area with pine afforestation (Richter and Markewitz, 2001). The findings are also in agreement  
270 with results from an incubation study by Fontaine et al., (2007) which showed that the deep soil can have a



271 significant dynamic component. Baisden et al., (2007) also found indications of a deep dynamic pool using  
272 modeling on  $^{14}\text{C}$  time-series on the bulk level on a New Zealand soil under stable pastoral management.

273

#### 274 **4.1.2 Carbon dynamics reflect soil-specific characteristics at depth**

275 Bulk carbon turnover for the top and deeper soil fall in the range of prior observations and models, although the  
276 data for the latter category is sparse (Scharpenseel and Becker-Heidelmann, 1989; Paul et al., 1997; Schmidt et  
277 al., 2011; Mills et al., 2013; Braakhekke et al., 2014). The carbon turnover is related to soil-specific  
278 characteristics. The slower turnover of hydromorphic as compared to non-hydromorphic soils is likely due to  
279 increased waterlogging and limited aerobicity (Hagedorn et al., 2001) which is conducive to slow turnover and  
280 enhanced carbon accumulation. The WEOC turns over up to an order of magnitude faster than the bulk and  
281 mirrors these trends, indicating that it indeed is a more dynamic pool (Hagedorn et al., 2004; Lechleitner et al.,  
282 2016). Results also reflect known horizon-specific dynamics for certain soil types, particularly in the deep soil.  
283 The hydromorphic Podsol at Beatenberg shows specific pedogenetic features such as an illuviation layer with an  
284 enrichment in humus and iron in the deeper soil (Walther et al., 2003) where turnover of bulk and WEOC is  
285 faster and stocks are higher than in the elluvial layer above (Fig. 5). This is likely due to the input of younger  
286 carbon via leaching of dissolved organic carbon. The non-hydromorphic Luvisols are marked by an enrichment  
287 of clay in the deeper soil, which can enhance carbon stabilization (Lutzow et al., 2006). This also reflected in  
288 the turnover time of the 60-80 cm layer in the Othmarsingen Luvisol – in this clay-enriched depth interval  
289 (Walther et al., 2003), turnover is relatively slow as compared to the other (colder) non-hydromorphic soils  
290 (Fig. 5).

291

#### 292 **4.1.3 Sizeable dynamic pool at depth & implications for carbon transport**

293 The  $^{14}\text{C}$  time series modelling indicate that the size of the dynamic pool can be large, even at greater depth than  
294 it was observed by other  $^{14}\text{C}$  time-series (Richter and Markewitz, 2001; Baisden and Parfitt, 2007; Koarashi et  
295 al., 2012). The two-pool modelling indicates that the size of dynamic pool in the deep soil can be upwards of  
296 ~14%. A deep dynamic pool is consistent with findings of a  $^{13}\text{C}$  tracer experiment by Hagedorn et al., (2001)  
297 that shows with that relatively young (<4 years) carbon can be rapidly incorporated in the top soil (20% new C  
298 at 0-20 cm depth) but also in the deep soil (50 cm). In our study, the illuvial horizon of the Podzol stands out  
299 again with a higher amount of the dynamic fraction than the elluvial horizon above. Rumpel and Kögel-Knabner  
300 (2011) have highlighted the importance of the poorly understood deep soil carbon stocks and a significant  
301 dynamic pool in the deep soil could imply that carbon is more vulnerable than initially suspected. One major  
302 input pathway of younger C into deeper soils is the leaching of DOC (Kaiser and Kalbitz, 2012; Sanderman and  
303 Amundson, 2009). Here, we have measured WEOC – likely primarily composed of microbial metabolites  
304 (Hagedorn et al., 2004) – carrying a younger  $^{14}\text{C}$  signature than bulk SOM and thus, representing a translocator  
305 of fresh carbon to the deep soil. In addition to WEOC, roots and associated mycorrhizal communities may also  
306 provide a substantial input of new C into soils in deeper soils (Rasse et al., 2005). Considering the non-  
307 hydromorphic soils alone, the size of the dynamic pool increases with site elevation and cooler MAT. This is  
308 consistent with findings of Budge et al., (2011) and Leifeld et al., (2009) that grassland soils at higher elevation  
309 have larger labile SOM pools.

310





#### 311 4.2 Contribution of petrogenic carbon

312 Our results on deep soil carbon suggest the presence of pre-aged or  $^{14}\text{C}$ -dead (fossil), pre-interglacial carbon in  
313 the Alptal (Gleysol) and Lausanne (Cambisol) profiles, implying that a component of soil carbon is not  
314 necessarily linked to recent (< millennial) terrestrial productivity and instead constitutes part of the long-term  
315 (geological) carbon cycle (> millions of years). In the case of the Gleysol in Alptal, the  $^{14}\text{C}$ -depleted material  
316 could be derived from the poorly consolidated sedimentary rocks (Flysch) in the region (Hagedorn et al., 2001a;  
317 Schleppei et al., 1998; Smith et al., 2013), whereas carbon present in glacial deposits and molasse may contribute  
318 in deeper soils at the Lausanne (Cambisol) site. The potential contribution of fossil carbon was estimated using a  
319 mixing model using the signature of a soil without fossil carbon, the signature of fossil carbon and the measured  
320 values (SI Table 4). Fossil carbon contribution in the Alptal profile between 80-100 cm (Fig. 6, SI Table 4) is  
321 estimated at ~40 %. Below one meter at Lausanne site the petrogenic percentage ranges from ~20% at 145 cm  
322 up to ~80 % at 310 cm depth (Fig. 6, SI Table 4).

323 Other studies analyzing soils have observed the significant presence of petrogenic (geogenic in soil  
324 science terminology) in loess-based soils (Helfrich et al., 2007; Paul et al., 2001). Our results suggest that pre-  
325 glacial carbon may comprise a dominant component of deep soil organic matter in several cases, resulting in an  
326 apparent increase in the average age (and decrease in turnover) of carbon in these soils. Hemingway et al.,  
327 (2018) have highlighted that fossil carbon oxidized in soils can lead to significant additional  $\text{CO}_2$  emissions.  
328 Therefore, the potential of soils to ‘activate’ fossil petrogenic carbon should be considered when evaluating the  
329 soil carbon sequestration potential.

330

#### 331 4.3 Controls on carbon dynamics and cycling

332 In order to examine the effects of potential drivers on soil C turnover, stocks and the size of the dynamic pool,  
333 we explore correlations between a number of available factors which have previously been proposed, such as  
334 texture, geology, precipitation, temperature and soil moisture (Doetterl et al., 2015; McFarlane et al., 2013;  
335 Nussbaum et al., 2014; Seneviratne et al., 2010; van der Voort et al., 2016). The vegetation-induced lag does not  
336 strongly impact turnover times except in the organic layer and in the top 5 cm of the mineral soil (SI Fig. 2).  
337 From examination of data for all samples it emerges that C turnover does not exhibit a consistent correlation  
338 with any specific climatological or physico-chemical factor. This implies that no single mechanism  
339 predominates and/or that there is a combined impact of geology and precipitation as these soil-forming factors  
340 affect grain size distribution, water regime and mass transport in soils. Exploring potential relationships in  
341 greater detail, we see that carbon stocks in the top soil and deep soil as well as turnover time is positively related  
342 to MAP, which could be linked to waterlogging and anaerobic conditions even in upland soils leading to a lower  
343 decomposition and thus to a higher build-up of organic material (Keiluweit et al., 2015). Our results are  
344 supported by the findings based on >1000 forest sites that precipitation exerts a strong effect on soil C stocks  
345 across Switzerland (Gosheva et al., 2017; Nussbaum et al., 2014). Turnover in both top and deep soil was most  
346 closely correlated with texture. The positive correlation of top soil turnover with grain size and negative  
347 correlation with the amount of silt-sized particles reflects lower stabilization in larger-grained soils as opposed  
348 to clay-rich soils with a higher and more reactive surface area (Rumpel and Kogel-Knabner, 2011). The  
349 modeled size of the dynamic pool is mostly related to precipitation and texture. It correlates positively with  
350 MAP and clay content and negatively with sand content. This correlation could be because sandier soils offer



351 less reactive surfaces for SOM stabilization as opposed to clay-rich soils (Lutzow et al., 2006). Additionally,  
352 wetter conditions inhibit SOM breakdown. Overall, geology seems to impact the carbon cycling in three key  
353 ways. Firstly, when petrogenic carbon is present in the bedrock from shale or reworked shale (Schleppi et al.,  
354 1998; Walther et al., 2003), fossil carbon contributes to soil carbon. Secondly, porosity of underlying bedrock  
355 either prevents or induces waterlogging which in turn affects turnover. Thirdly, the initial components of the  
356 bedrock (i.e. silt-sizes layers in an alluvial fan) influence the final grain size distribution and mineralogy (SI Fig.  
357 3, Table 3), which is also reflected in the bulk and pool-specific turnover. Within the limited geographic and  
358 temporal scope of this paper, we hypothesize that for soil carbon stocks and their turnover, temperature is not  
359 the dominant driver, which has been concluded by some (Giardina and Ryan, 2000) but refuted by others  
360 (Davidson et al., 2000; Feng et al., 2008). The only climate-related driver which appears to be significant is  
361 precipitation.

362

#### 363 4.4 Modular robust numerical optimization

364 The numerical approach used here builds on previous work concerning turnover modeling of bomb-radiocarbon  
365 dominated samples (Herold et al., 2014; Solly et al., 2013; Torn et al., 2009) and the approach used in numerous  
366 time-series analysis with box modeling using Excel (Schrumpf and Kaiser, 2015) or Excel solver (Baisden et al.,  
367 2013; Prior et al., 2007). However certain modifications were made in order to (i) provide objective repeatable  
368 estimates, (ii) incorporate the WEOC as a sub-pool of C, and (iii) identify samples impacted by petrogenic (also  
369 called geogenic) carbon. Identifying petrogenic carbon in the deep soil is important considering the large carbon  
370 stocks in deep soils (Rumpel and Kogel-Knabner, 2011) and the wider relevance of petrogenically-derived  
371 carbon in the global carbon cycle (Galy et al., 2008). This approach is modular and could be adapted in the  
372 future to identify the correct turnover for time-series  $^{14}\text{C}$  data, which is becoming increasingly important with  
373 the falling bomb-peak (Graven, 2015).

374

#### 375 5 Conclusion

376 Time-series radiocarbon ( $^{14}\text{C}$ ) analyses of soil carbon across a climatic range reveals recent bomb-derived  
377 radiocarbon in both upper and deeper bulk soil, implying the presence of a rapidly turning over pool at depth.  
378 Pool-specific time-series measurements of the WEOC indicate this is a more dynamic pool which is consistently  
379 more enriched in radiocarbon than the bulk. The modeled size of the dynamic fraction is non-negligible even in  
380 the deep soil (~0.14-0.46). This could imply that a component of the deep soil carbon could be more dynamic  
381 than previously thought.

382 The interaction between precipitation and geology appears to be the main control on carbon dynamics  
383 rather than site temperature. Carbon turnover in non-hydromorphic soils is relatively similar (decades to  
384 centuries) despite dissimilar climatological conditions. Hydromorphic soils have turnover times which are up to  
385 an order of magnitude slower. These trends are mirrored in the dynamic WEOC pool, suggesting that in sandy,  
386 non-waterlogged (aerobic) soils the transport of relatively modern (bomb-derived) carbon into the deep soil  
387 and/or the microbial processing is enhanced as compared to fine-grained waterlogged (anaerobic) soils.

388 Model results indicate certain soils contain significant quantities of pre-glacial or petrogenic (bedrock-  
389 derived) carbon in the deeper part of their profiles. This implies that soils not only sequester “modern” but can  
390 rather also mobilize and potentially metabolize “fossil” or geogenic carbon.



391 Overall, these time-series  $^{14}\text{C}$  bulk and pool-specific data, coupled to a robust numerical modeling  
392 approach, provide novel constraints on soil carbon dynamics in surface and deeper soils for a range of  
393 ecosystems.  
394

395 **Acknowledgements**

396 We would like to acknowledge the SNF NRP68 *Soil as a Resource* program for funding this project (SNF  
397 406840\_143023/11.1.13-31.12.15). We would like to thank various members of the Laboratory of Ion Beam  
398 Physics and Biogeoscience group for their help with the analyses, in particular Lukas Wacker. We thank Roger  
399 Köchli for his crucial help in the field which enabled an effective time-series comparison and for his help with  
400 subsequent analyses. We thank Emily Solly and Sia Gosheva for their valuable insights, Claudia Zell for her  
401 help on the project and in the field, Peter Waldner for facilitating the fieldwork, and Elisabeth Graf-Pannatier  
402 for her insights on soil moisture. The 2014 field campaign would not have been possible without the help of  
403 Thomas Blattmann, Lukas Oesch, Markus Vaas and Niko Westphal. Thanks to Stephane Beaussier for the  
404 insights into numerical modeling. Also thanks to Nadine Keller and Florian Neugebauer for their help in the lab.  
405 Last but not least, thanks to Thomas Bär for summarizing ancillary pH data. Data supporting this paper is  
406 provided in a separate data Table.

407

408 **References**

- 409 Angst, G., John, S., Mueller, C. W., Kögel-Knabner, I. and Rethemeyer, J.: Tracing the sources and spatial  
410 distribution of organic carbon in subsoils using a multi-biomarker approach, *Sci. Rep.*, 6(1), 29478,  
411 doi:10.1038/srep29478, 2016.
- 412 Von Arx, G., Graf Pannatier, E., Thimonier, A. and Rebetez, M.: Microclimate in forests with varying leaf area  
413 index and soil moisture: Potential implications for seedling establishment in a changing climate, *J. Ecol.*, 101(5),  
414 1201–1213, doi:10.1111/1365-2745.12121, 2013.
- 415 Baisden, W. T. and Parfitt, R. L.: Bomb <sup>14</sup>C enrichment indicates decadal C pool in deep soil?,  
416 *Biogeochemistry*, 85(1), 59–68, doi:10.1007/s10533-007-9101-7, 2007.
- 417 Baisden, W. T., Parfitt, R. L., Ross, C., Schipper, L. A. and Canessa, S.: Evaluating 50 years of time-series soil  
418 radiocarbon data : towards routine calculation of robust C residence times, *Biogeochemistry*, 112, 129–137,  
419 doi:10.1007/s10533-011-9675-y, 2013.
- 420 Batjes, N. H.: Total carbon and nitrogen in the soils of the world, *Eur. J. Soil Sci.*, 47(June), 151–163, 1996.
- 421 Braakhekke, M. C., Beer, C., Schrupf, M., Ekici, A., Ahrens, B., Hoosbeek, M. R., Kruijt, B., Kabat, P. and  
422 Reichstein, M.: The use of radiocarbon to constrain current and future soil organic matter turnover and transport  
423 in a temperate forest, *J. Geophys. Res. Biogeosciences*, 119(3), 372–391, doi:10.1002/2013JG002420, 2014.
- 424 Budge, K., Leifeld, J., Hiltbrunner, E. and Fuhrer, J.: Alpine grassland soils contain large proportion of labile  
425 carbon but indicate long turnover times, *Biogeosciences*, 8(7), 1911–1923, doi:10.5194/bg-8-1911-2011, 2011.
- 426 Carvalhais, N., Forkel, M., Khomik, M., Bellarby, J., Jung, M., Migliavacca, M., Mu, M., Saatchi, S., Santoro,  
427 M., Thurner, M., Weber, U., Ahrens, B., Beer, C., Cescatti, A., Randerson, J. T., Reichstein, M., Mu, M.,  
428 Saatchi, S., Santoro, M., Thurner, M., Weber, U., Ahrens, B., Beer, C., Cescatti, A., Randerson, J. T.,  
429 Reichstein, M., Mu, M., Saatchi, S., Santoro, M., Thurner, M., Weber, U., Ahrens, B., Beer, C., Cescatti, A.,  
430 Randerson, J. T. and Reichstein, M.: Global covariation of carbon turnover times with climate in terrestrial  
431 ecosystems, *Nature*, 514(7521), 213–217, doi:10.1038/nature13731, 2014.
- 432 Crowther, T., Todd-Brown, K., Rowe, C., Wieder, W., Carey, J., Machmuller, M., Snoek, L., Fang, S., Zhou,  
433 G., Allison, S., Blair, J., Bridgman, S., Burton, A., Carrillo, Y., Reich, P., Clark, J., Classen, A., Dijkstra, F.,  
434 Elberling, B., Emmett, B., Estiarte, M., Frey, S., Guo, J., Harte, J., Jiang, L., Johnson, B., Kröel-Dulay, G.,  
435 Larsen, K., Laudon, H., Lavalley, J., Luo, Y., Lupascu, M., Ma, L., Marhan, S., Michelsen, A., Mohan, J., Niu,  
436 S., Pendall, E., Penuelas, J., Pfeifer-Meister, L., Poll, C., Reinsch, S., Reynolds, L., Schmidh, I., Sistla, S.,  
437 Sokol, N., Templer, P., Treseder, K., Welker, J. and Bradford, M.: Quantifying global soil C losses in response  
438 to warming, *Nature*, 540(1), 104–108, doi:10.1038/nature20150, 2016.
- 439 Davidson, E. A. and Janssens, I. A.: Temperature sensitivity of soil carbon decomposition and feedbacks to  
440 climate change., *Nature*, 440(7081), 165–73 [online] Available from:  
441 <http://www.ncbi.nlm.nih.gov/pubmed/16525463>, 2006.
- 442 Davidson, E. A., Trumbore, S. E. and Amundson, R.: Soil warming and organic carbon content., *Nature*,  
443 408(December), 789–790, doi:10.1038/35048672, 2000.
- 444 Doetterl, S., Stevens, A., Six, J., Merckx, R., Oost, K. Van, Pinto, M. C., Casanova-katny, A., Muñoz, C.,  
445 Boudin, M., Venegas, E. Z. and Boeckx, P.: Soil carbon storage controlled by interactions between  
446 geochemistry and climate, *Nat. Geosci.*, 8(August), 1–4, doi:10.1038/NGEO2516, 2015.
- 447 Etzold, S., Waldner, P., Thimonier, A., Schmitt, M. and Dobbertin, M.: Tree growth in Swiss forests between



- 448 1995 and 2010 in relation to climate and stand conditions: Recent disturbances matter, *For. Ecol. Manage.*, 311,  
449 41–55 [online] Available from: <http://linkinghub.elsevier.com/retrieve/pii/S0378112713003393> (Accessed 3  
450 June 2014), 2014.
- 451 Feng, X., Simpson, A. J., Wilson, K. P., Williams, D. D. and Simpson, M. J.: Increased cuticular carbon  
452 sequestration and lignin oxidation in response to soil warming, *Nat. Geosci.*, 1(December), 836–839, 2008.
- 453 Fierer, N., Schimel, J. P. and Holden, P. A.: Variations in microbial community composition through two soil  
454 depth profiles, *Soil Biol. Biochem.*, 35, 167–176, 2003.
- 455 Fontaine, S., Barot, S., Barré, P., Bdioui, N., Mary, B. and Rumpel, C.: Stability of organic carbon in deep soil  
456 layers controlled by fresh carbon supply., *Nature*, 450, 277–280, 2007.
- 457 Fröberg, M., Tipping, E., Stendahl, J., Clarke, N. and Bryant, C.: Mean residence time of O horizon carbon  
458 along a climatic gradient in Scandinavia estimated by  $^{14}\text{C}$  measurements of archived soils, *Biogeochemistry*,  
459 104(1–3), 227–236 [online] Available from: <http://link.springer.com/10.1007/s10533-010-9497-3> (Accessed 2  
460 August 2013), 2010.
- 461 Galy, V., Beyssac, O., France-Lanord, C. and Eglinton, T. I.: Recycling of graphite during Himalayan erosion: a  
462 geological stabilization of carbon in the crust, *Science (80-. )*, 322(November), 943–945,  
463 doi:10.1126/science.1161408, 2008.
- 464 Giardina, C. P. and Ryan, M. G.: Evidence that decomposition rates of organic carbon in mineral soil do not  
465 vary with temperature, *Nature*, 404(6780), 858–861, doi:10.1038/35009076, 2000.
- 466 Gosheva, S., Walthert, L., Niklaus, P. A., Zimmermann, S., Gimmi, U. and Hagedorn, F.: Reconstruction of  
467 Historic Forest Cover Changes Indicates Minor Effects on Carbon Stocks in Swiss Forest Soils, *Ecosystems*,  
468 (C), doi:10.1007/s10021-017-0129-9, 2017.
- 469 Graven, H. D.: Impact of fossil fuel emissions on atmospheric radiocarbon and various applications of  
470 radiocarbon over this century, *Proc. Natl. Acad. Sci.*, (Early Edition), 1–4, doi:10.1073/pnas.1504467112, 2015.
- 471 Hagedorn, F., Bucher, J. B. and Schleppl, P.: Contrasting dynamics of dissolved inorganic and organic nitrogen  
472 in soil and surface waters of forested catchments with Gleysols, *Geoderma*, 100(1–2), 173–192,  
473 doi:10.1016/S0016-7061(00)00085-9, 2001a.
- 474 Hagedorn, F., Maurer, S., Egli, P., Blaser, P., Bucher, J. B. and Siegw: Carbon sequestration in forest soils :  
475 effects of soil type , atmospheric  $\text{CO}_2$  enrichment , and N deposition, *Eur. J. Soil Sci.*, 52(December), 2001b.
- 476 Hagedorn, F., Saurer, M. and Blaser, P.: A  $^{13}\text{C}$  tracer study to identify the origin of dissolved organic carbon in  
477 forested mineral soils, *Eur. J. Soil Sci.*, 55(1), 91–100 [online] Available from:  
478 <http://doi.wiley.com/10.1046/j.1365-2389.2003.00578.x> (Accessed 26 September 2013), 2004.
- 479 He, Y., Trumbore, S. E., Torn, M. S., Harden, J. W., Vaughn, L. J. S., Allison, S. D. and Randerson, J. T.:  
480 Radiocarbon constraints imply reduced carbon uptake by soils during the 21st century, *Science (80-. )*,  
481 353(6306), 1419–1424, 2016.
- 482 Helfrich, M., Flessa, H., Mikutta, R., Dreves, A. and Ludwig, B.: Comparison of chemical fractionation  
483 methods for isolating stable soil organic carbon pools, *Eur. J. Soil Sci.*, 58(6), 1316–1329, doi:10.1111/j.1365-  
484 2389.2007.00926.x, 2007.
- 485 Hemingway, J.: Microbial oxidation of lithospheric organic carbon in rapidly eroding tropical mountain soils,  
486 *Science (80-. )*, (April), doi:10.1126/science.aao6463, 2018.
- 487 Herold, N., Schöning, L., Michalzik, B., Trumbore, S. E. and Schrupf, M.: Controls on soil carbon storage and  
488 turnover in German landscapes, *Biogeochemistry*, 119(1–3), 435–451, doi:x, 2014.
- 489 Hicks Pries, C. E., Castanha, C., Porras, R. C. and Torn, M. S.: The whole-soil carbon flux in response to  
490 warming, *Science (80-. )*, 1319(March), 1–9, 2017.
- 491 Ivy-Ochs, S., Kerschner, H., Maisch, M., Christl, M., Kubik, P. W. and Schluchter, C.: Latest Pleistocene and  
492 Holocene glacier variations in the European Alps, *Quat. Sci. Rev.*, 28(21–22), 2137–2149,  
493 doi:10.1016/j.quascirev.2009.03.009, 2009.
- 494 Jobbagy, E. G. and Jackson, R. : Ther vertical distribution of soil organic carbon an its relation to climate and  
495 vegetation, *Ecol. Appl.*, 10(April), 423–436, 2000.
- 496 Kaiser, K. and Kalbitz, K.: Cycling downwards - dissolved organic matter in soils, *Soil Biol. Biochem.*, 52, 29–  
497 32, doi:10.1016/j.soilbio.2012.04.002, 2012.
- 498 Keiluweit, M., Bougoure, J. J., Nico, P. S., Pett-Ridge, J., Weber, P. K. and Kleber, M.: Mineral protection of  
499 soil carbon counteracted by root exudates, *Nat. Clim. Chang.*, 5(6), doi:10.1038/nclimate2580, 2015.
- 500 Klute, A.: Methods of soil analysis, Part 1: Physical and Mineralogical Methods, 2nd ed., Agronomy  
501 Monograph No 9, Madison WI., 1986.
- 502 Koarashi, J., Hockaday, W. C., Masiello, C. a. and Trumbore, S. E.: Dynamics of decadal cycling carbon in  
503 subsurface soils, *J. Geophys. Res. Biogeosciences*, 117(3), 1–13, doi:10.1029/2012.JG002034, 2012.
- 504 Komada, T., Anderson, M. R. and Dorfmeier, C. L.: Carbonate removal from coastal sediments for the  
505 determination of organic carbon and its isotopic signatures ,  $\delta^{13}\text{C}$  and  $\Delta^{14}\text{C}$  : comparison of fumigation and  
506 direct acidification by hydrochloric acid, *Limnol. Oceanogr. Methods*, (6), 254–262, 2008.
- 507 Lang, S. Q., McIntyre, C. P., Bernasconi, S. M., Früh-Green, G. L., Voss, B. M., Eglinton, T. I. and Wacker, L.:



- 508 Rapid 14C Analysis of Dissolved Organic Carbon in Non-Saline Waters, *Radiocarbon*, 58(3), 1–11,  
509 doi:10.1017/RDC.2016.17, 2016.
- 510 Lechleitner, F. A., Baldini, J. U. L., Breitenbach, S. F. M., Fohlmeister, J., McIntyre, C., Goswami, B.,  
511 Jamieson, R. A., van der Voort, T. S., Pruger, K., Marwan, N., Culleton, B. J., Kennett, D. J., Asmerom, Y.,  
512 Polyak, V. and Eglinton, T. I.: Hydrological and climatological controls on radiocarbon concentrations in a  
513 tropical stalagmite, *Geochim. Cosmochim. Acta*, doi:10.1016/j.gca.2016.08.039, 2016.
- 514 Leifeld, J., Zimmermann, M., Fuhrer, J. and Conen, F.: Storage and turnover of carbon in grassland soils along  
515 an elevation gradient in the Swiss Alps, *Glob. Chang. Biol.*, 15(3), 668–679, doi:10.1111/j.1365-  
516 2486.2008.01782.x, 2009.
- 517 Levin, I., Naegler, T., Kromer, B., Diehl, M., Francey, R. J., Gomez-Pelaez, A. J., Steele, L. P., Wagenbach, D.,  
518 Weller, R. and Worthy, D. E.: Observations and modelling of the global distribution and long-term trend of  
519 atmospheric 14CO<sub>2</sub>, *Tellus, Ser. B Chem. Phys. Meteorol.*, 62(1), 26–46, doi:10.1111/j.1600-  
520 0889.2009.00446.x, 2010.
- 521 Lutzow, M. V., Kogel-Knabner, I., Ekschmitt, K., Matzner, E., Guggenberger, G., Marschner, B. and Flessa, H.:  
522 Stabilization of organic matter in temperate soils: mechanisms and their relevance under different soil  
523 conditions - a review, *Eur. J. Soil Sci.*, 57, 426–445 [online] Available from:  
524 <http://doi.wiley.com/10.1111/j.1365-2389.2006.00809.x>, 2006a.
- 525 Lutzow, M. V., Kogel-Knabner, I., Ekschmitt, K., Matzner, E., Guggenberger, G., Marschner, B. and Flessa, H.:  
526 Stabilization of organic matter in temperate soils: mechanisms and their relevance under different soil  
527 conditions - a review, *Eur. J. Soil Sci.*, 57(4), 426–445, doi:10.1111/j.1365-2389.2006.00809.x, 2006b.
- 528 McFarlane, K. J., Torn, M. S., Hanson, P. J., Porras, R. C., Swanston, C. W., Callahan, M. A. and Guilderson,  
529 T. P.: Comparison of soil organic matter dynamics at five temperate deciduous forests with physical  
530 fractionation and radiocarbon measurements, *Biogeochemistry*, 112(1–3), 457–476, doi:10.1007/s10533-012-  
531 9740-1, 2013.
- 532 McIntyre, C. P., Wacker, L., Haghypour, N., Blattmann, T. M., Fahrni, S., Usman, M., Eglinton, T. I. and Synal,  
533 H.-A.: Online 13C and 14C Gas Measurements by EA-IRMS-AMS at ETH Zürich, *Radiocarbon*, 2(November  
534 2015), 1–11, doi:10.1017/RDC.2016.68, 2016.
- 535 Melillo, J. M., Steudler, P. a, Aber, J. D., Newkirk, K., Lux, H., Bowles, F. P., Catricala, C., Magill, A., Ahrens,  
536 T. and Morrisseau, S.: Soil warming and carbon-cycle feedbacks to the climate system., *Science*, 298(5601),  
537 2173–6 [online] Available from: <http://www.ncbi.nlm.nih.gov/pubmed/12481133> (Accessed 21 January 2014),  
538 2002.
- 539 Mills, R. T. E., Tipping, E., Bryant, C. L. and Emmett, B. a.: Long-term organic carbon turnover rates in natural  
540 and semi-natural topsoils, *Biogeochemistry*, 118(1), 257–272 [online] Available from:  
541 <http://link.springer.com/10.1007/s10533-013-9928-z> (Accessed 18 December 2013a), 2013.
- 542 Nussbaum, M., Papritz, A., Baltensweiler, A. and Walthert, L.: Estimating soil organic carbon stocks of Swiss  
543 forest soils by robust external-drift kriging, *Geosci. Model Dev.*, 7(3), 1197–1210, doi:10.5194/gmd-7-1197-  
544 2014, 2014.
- 545 Paul, E. A., Collins, H. P. and Leavitt, S. W.: Dynamics of resistant soil carbon of midwestern agricultural soils  
546 measured by naturally occurring 14C abundance, *Geoderma*, 104(3–4), 239–256, doi:10.1016/S0016-  
547 7061(01)00083-0, 2001.
- 548 Paul, E. A., Follett, R. F., Leavitt, W. S., Halvorson, A., Petersen, G. A. and Lyon, D. J.: Radiocarbon Dating  
549 for Determination of Soil Organic Matter Pool Sizes and Dynamics, *Soil Sci. Soc. Am. J.*, 61(4), 1058–1067,  
550 1997.
- 551 Prietzel, J., Zimmermann, L., Schubert, A. and Christophel, D.: Organic matter losses in German Alps forest  
552 soils since the 1970s most likely caused by warming, *Nat. Geosci.*, 9(July), doi:10.1038/ngeo2732, 2016.
- 553 Prior, C. A., Baisden, W. T., Bruhn, F. and Neff, J. C.: Using a soil chronosequence to identify soil fractions for  
554 understanding and modeling soil carbon dynamics in New Zealand, *Radiocarbon*, 49(2), 1093–1102, 2007.
- 555 Rasse, D. P., Rumpel, C. and Dignac, M.-F.: Is soil carbon mostly root carbon? Mechanisms for a specific  
556 stabilisation, *Plant Soil*, 269(1–2), 341–356 [online] Available from: <http://link.springer.com/10.1007/s11104-004-0907-y>, 2005.
- 557 Rethemeyer, J., Kramer, C., Gleixner, G., John, B., Yamashita, T., Flessa, H., Andersen, N., Nadeau, M. and  
558 Grootes, P. M.: Transformation of organic matter in agricultural soils : radiocarbon concentration versus soil  
559 depth, *Geoderma*, 128, 94–105, doi:10.1016/j.geoderma.2004.12.017, 2005.
- 560 Richter, D. D. and Markewitz, D.: *Understanding Soil Change*, Cambridge University Press, Cambridge., 2001.
- 561 Rumpel, C. and Kogel-Knabner, I.: Deep soil organic matter—a key but poorly understood component of  
562 terrestrial C cycle, *Plant Soil*, 338, 143–158, 2011.
- 563 Sanderman, J. and Amundson, R.: A comparative study of dissolved organic carbon transport and stabilization  
564 in California forest and grassland soils, *Biogeochemistry*, 92(1–2), 41–59, doi:10.1007/s10533-008-9249-9,  
565 2009.
- 566 Scharpenseel, H. W. and Becker-Heidelmann, P.: Shifts in 14C patterns of soil profiles due to bomb carbon,  
567



- 568 including effects of morphogenetic and turbation processes, *Radiocarbon*, 31(3), 627–636, 1989.
- 569 Schaub, M., Dobbertin, M., Kräuchi, N. and Dobbertin, M. K.: Preface-long-term ecosystem research:
- 570 Understanding the present to shape the future, *Environ. Monit. Assess.*, 174(1–4), 1–2, doi:10.1007/s10661-010-  
571 1756-1, 2011.
- 572 Schimel, D. S., House, J. I., Hibbard, K. a, Bousquet, P., Ciais, P., Peylin, P., Braswell, B. H., Apps, M. J.,  
573 Baker, D., Bondeau, A., Canadell, J., Churkina, G., Cramer, W., Denning, a S., Field, C. B., Friedlingstein, P.,  
574 Goodale, C., Heimann, M., Houghton, R. a, Melillo, J. M., Moore, B., Murdiyarso, D., Noble, I., Pacala, S. W.,  
575 Prentice, I. C., Raupach, M. R., Rayner, P. J., Scholes, R. J., Steffen, W. L. and Wirth, C.: Recent patterns and  
576 mechanisms of carbon exchange by terrestrial ecosystems., *Nature*, 414(6860), 169–72 [online] Available from:  
577 <http://www.ncbi.nlm.nih.gov/pubmed/11700548>, 2001.
- 578 Schleppe, P., Muller, N., Feyen, H., Papritz, A., Bucher, J. B. and Fluehler, H.: Nitrogen budgets of two small  
579 experimental forested catchments at Alptal, Switzerland, *For. Ecol. Manage.*, 127(101), 177–185, 1998.
- 580 Schmidt, M. W. I., Torn, M. S., Abiven, S., Dittmar, T., Guggenberger, G., Janssens, I. a, Kleber, M., Kögel-  
581 Knabner, I., Lehmann, J., Manning, D. a C., Nannipieri, P., Rasse, D. P., Weiner, S. and Trumbore, S. E.:  
582 Persistence of soil organic matter as an ecosystem property., *Nature*, 478(7367), 49–56 [online] Available from:  
583 <http://www.ncbi.nlm.nih.gov/pubmed/21979045> (Accessed 21 January 2014), 2011.
- 584 Schrumpf, M. and Kaiser, K.: Large differences in estimates of soil organic carbon turnover in density fractions  
585 by using single and repeated radiocarbon inventories, *Geoderma*, 239–240, 168–178 [online] Available from:  
586 <http://linkinghub.elsevier.com/retrieve/pii/S0016706114003577>, 2015.
- 587 Schrumpf, M., Kaiser, K., Guggenberger, G., Persson, T., Kögel-Knabner, I. and Schulze, E.-D.: Storage and  
588 stability of organic carbon in soils as related to depth, occlusion within aggregates, and attachment to minerals,  
589 *Biogeosciences*, 10, 1675–1691, 2013.
- 590 Seneviratne, S. I., Corti, T., Davin, E. L., Hirschi, M., Jaeger, E. B., Lehner, I., Orlowsky, B. and Teuling, A. J.:  
591 Investigating soil moisture-climate interactions in a changing climate: A review, *Earth-Science Rev.*, 99(3–4),  
592 125–161, doi:10.1016/j.earscirev.2010.02.004, 2010.
- 593 Sierra, C. A., Muller, M., Metzler, H., Manzoni, S. and Trumbore, S. E.: The muddle of ages, turnover, transit,  
594 and residence times in the carbon cycle, *Glob. Chang. Biol.*, 1–11, doi:10.1111/gcb.13556, 2016.
- 595 Smith, J. C., Galy, A., Hovius, N., Tye, A. M., Turowski, J. M. and Schleppe, P.: Runoff-driven export of  
596 particulate organic carbon from soil in temperate forested uplands, *Earth Planet. Sci. Lett.*, 365, 198–208,  
597 doi:10.1016/j.epsl.2013.01.027, 2013.
- 598 Solly, E., Schöning, I., Boch, S., Müller, J., Socher, S. a., Trumbore, S. E. and Schrumpf, M.: Mean age of  
599 carbon in fine roots from temperate forests and grasslands with different management, *Biogeosciences*, 10(7),  
600 4833–4843, doi:10.5194/bg-10-4833-2013, 2013.
- 601 Torn, M. S., Swanston, C. W., Castanha, C. and Trumbore, S. E.: Storage and turnover of organic matter in soil,  
602 in *Biophysico-Chemical Processes Involving Natural Nonliving Organic Matter in Environmental Systems*,  
603 edited by N. Senesi, B. Xing, and P. M. Huang, p. 54, John Wiley & Sons, Inc., 2009.
- 604 Trumbore, S. E. and Czimczik, C. I.: Geology. An uncertain future for soil carbon., *Science*, 321, 1455–1456,  
605 2008.
- 606 van der Voort, T. S., Hagedorn, F., McIntyre, C., Zell, C., Walthert, L. and Schleppe, P.: Variability in 14C  
607 contents of soil organic matter at the plot and regional scale across climatic and geologic gradients,  
608 *Biogeosciences*, 13(January), 3427–3439, doi:10.5194/bg-2015-649, 2016.
- 609 Wacker, L., Bonani, G., Friedrich, M., Hajdas, I., Kromer, B., Němec, M., Ruff, M., Suter, M., Synal, H.-A. and  
610 Vockenhuber, C.: MICADAS: Routine and high-precision radiocarbon dating, *Radiocarbon*, 52(2), 252–262,  
611 2010.
- 612 Wacker, L., Němec, M. and Bourquin, J.: A revolutionary graphitisation system: Fully automated, compact and  
613 simple, *Nucl. Instruments Methods Phys. Res. Sect. B Beam Interact. with Mater. Atoms*, 268(7–8), 931–934  
614 [online] Available from: <http://linkinghub.elsevier.com/retrieve/pii/S0168583X09011161> (Accessed 2 August  
615 2013), 2009.
- 616 Walthert, L., Blaser, P., Lüscher, P., Luster, J. and Zimmermann, S.: Langfristige Waldökosystem-Forschung  
617 LWF in der Schweiz. Kernprojekt Bodenmatrix. Ergebnisse der ersten Erhebung 1994–1999., 2003.
- 618 Walthert, L., Graf Pannatier, E. and Meier, E. S.: Shortage of nutrients and excess of toxic elements in soils  
619 limit the distribution of soil-sensitive tree species in temperate forests, *For. Ecol. Manage.*, 297, 94–107,  
620 doi:10.1016/j.foreco.2013.02.008, 2013.
- 621 Walthert, L., Lüscher, P., Luster, J. and Peter, B.: Langfristige Waldökosystem- Forschung LWF. Kernprojekt  
622 Bodenmatrix. Aufnahmeanleitung zur ersten Erhebung 1994–1999, Swiss Federal Institute for Forest, Snow and  
623 Landscape Research WSL, Birmensdorf., 2002.
- 624
- 625
- 626



627 **Author contributions**

628 T.S. van der Voort planned, coordinated and executed the sampling strategy and sample collection, performed  
629 the analyses, conceptualized and optimized the model and processed resulting data. U. Mannu led the model  
630 development. F. Hagedorn lent his expertise on soil carbon cycling and soil properties. C. McIntyre facilitated  
631 and coordinated the radiocarbon measurements and associated data corrections. L. Walthert and P. Schleppe lent  
632 their expertise on the legacy sampling and provided data for the compositional analysis. N. Haghypour  
633 performed in isotopic and compositional measurements. T. Eglinton provided the conceptual framework and  
634 aided in the paper structure set-up. T.S. van der Voort prepared the manuscript with help of all co-authors.





**Tables**

**Table 1** Overview sampling locations and climatic and ecological parameters.

Location	Soil type	Geology	Latitude(N)/ Longitude (E)	Soil depth (m)	Depth waterlogging (m) <sup>1</sup>	Upper limit	Altitude (m a.s.l.)	Elevation MAT °C	MAP mm y <sup>-1</sup>	NPP g C m <sup>-2</sup> y <sup>-1</sup>
Othmarsingen <sup>1, 2, 3</sup>	Luvisol	Calcareous moraine	47°24'/8°14'	>1.9	2.5		467-500	9.2	1024	845
Lausanne <sup>1, 2, 3</sup>	Cambisol	Calcarous and moraine	46°34'/6°39'	>3.2	2.5		800-814	7.6	1134	824
Alptal <sup>1, 2, 3, 4</sup>	Gleysol	Flysch (carbon-holding sedimentary rock)	47°02'/8°43'	>1.0	0.1		1200	5.3	2126	347
Beatenberg <sup>1, 2, 3</sup>	Podzol	Sandstone	46°42'/7°46'	0.65	0.5		1178-1191	4.7	1163	302
Nationalpark <sup>1, 2, 3</sup>	Fluvisol	Calcareous alluvial fan	46°40'/10°14'	>1.1	2.5		1890-1907	1.3	864	111

<sup>1</sup> Walthert et al. (2003) <sup>2</sup>Eitzold et al., (2014) <sup>3</sup>Von Arx et al., (2013) <sup>4</sup>Krause et al., (2013) for Alptal data



**Table 2** Vegetation and soil data of the study sites. Soil water potential (hPa) are for 15 cm depth.

Location <sup>1</sup>	Deciduous tree species (%) <sup>3</sup>	Dominant species <sup>3</sup>	tree Inferred lag carbon fixation (y)	Organic layer Type <sup>1</sup>	Sand (%)	Silt (%)	Clay (%)	Soil water potential <sup>3</sup> (hPa)		
								5%	50%	95%
Othmarsingen	100	<i>Fagus sylvatica</i>	2	Mull	47	35	18	-577	-39	-9
Lausanne	80	<i>Fagus sylvatica</i>	3	Mull	47	34	19	-547	-49	-8
Alptal <sup>4</sup>	15	<i>Picea abies</i>	7	Mor to anmoor	6	48	46	-38	-13	+1
Beatenberg	0	<i>Picea abies</i>	8	Mor	86	11	3	-50	-14	+1
Nationalpark	0	<i>Pinus montana</i>	8	Moder	48	41	11	-388	-65	-13

<sup>1</sup>Walthert et al. (2003) <sup>2</sup>Eitzold et al., (2014), <sup>3</sup>Von Arx et al. (2013), <sup>4</sup>Krause et al., (2013)



**Table 3** Soil properties as well as carbon stocks and fluxes in 0-20, 20-60, and 60-100 cm depth of the study sites for the bulk and water-extractable organic carbon (WEOC).

Location	Depth interval (m)	pH <sup>1</sup>	CEC <sup>1</sup> (mmolc/kg)	Fe <sub>ex</sub> changeable (mmolc/kg)	Al <sub>ex</sub> changeable (mmolc/kg)	Sand content (%)	Silt content (%)	Clay content (%)	Carbon stock kgC/m <sup>2</sup>	Average turnover bulk (y)	Average turnover WEOC (y)
Othmarsingen <sup>1</sup>	0.0-0.2	4.4	62.2	0.15	42	46.8	35.5	17.6	4.84	162	35
	0.2-0.6	4.4	62.8	0.10	49	44.3	33.3	22.4	1.69	868	517
	0.6-0.8	4.9	99.5	0.06	41	46.7	28.4	25.0	0.28	3938	-
Lausanne <sup>1</sup>	0.0-0.2	4.5	60.8	0.13	43	49.2	32.6	18.2	3.24	298	77
	0.2-0.6	4.6	43.9	0	34	50.2	32.0	17.8	2.12	1197	586
	0.6-1.0	4.8	49.7	0	35	50.5	31.5	18.1	0.69	2242	1502 <sup>5</sup>
Alptal <sup>2,3,4</sup>	0.0-0.2	4.5	417	-	19	19.3	39.4	41.3	7.73	293	166
	0.2-0.6	4.7	340	-	14	4.90	47.0	48.1	7.24	2943	893 <sup>6</sup>
	0.6-1.0	4.7	340	-	-	-	-	-	6.54	5165	-
Beatenberg <sup>1</sup>	Organic layer	3.1	260.2	2.8	33	-	-	-	7.05	54	-
	0.0-0.2	4.0	35.6	1.7	18	84.9	12.4	2.7	3.65	1081	293
	0.2-0.6	4.1	23.1	0.40	17	83.2	12.3	4.6	4.10	1607	677
Nationalpark <sup>1</sup>	0.0-0.2	8.3	171.8	0.1	0.0	47.5	34.8	17.7	3.23	159	92
	0.2-0.6	8.8	106.3	0.0	0.0	61.9	32.5	5.7	0.36	612	214
	0.6-0.8	-	-	0.0	0.0	60.6	33.6	5.9	0.08	983	-

<sup>1</sup>Walther et al., 2002; Walther et al., 2003; <sup>2</sup>Fe and Al content (mmolc/kg) determined by NH<sub>4</sub>Cl extraction.

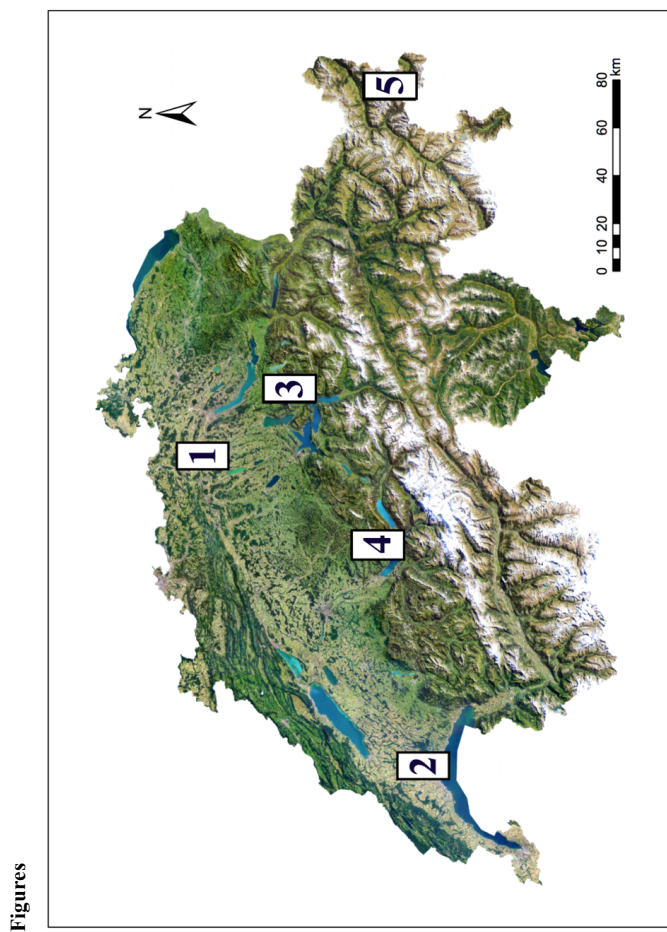
<sup>3</sup>For the 0.2-0.6 depth interval the CEC determined for 0.2-0.4 m was taken, and similarly for the depth interval 0.6-1.0 m the values for 0.6-0.8 m were taken in the case of Othmarsingen, Lausanne Beatenberg and Nationalpark.

<sup>4</sup>Knauss et al., 2004; <sup>5</sup>Dierksen et al., 1992; CEC determined (mmolc/kg), hydrogen lead and zinc ions were not included. Aluminium content determined by Lakeman method. CEC values for 0.2-0.4 m were extrapolated to 1 m. <sup>6</sup>Xu et al., 2009; <sup>7</sup>Depth to 0.8 m; <sup>8</sup>Depth to 0.4 m



**Table 4** Pearson correlations for averaged depth intervals for the top soil (0–20 cm, n=5) and deep soil (20–60 cm, n=5). Significance denoted with ; \* , \*\* or \*\*\* for respectively p-values smaller than 0.1 (marginally significant) 0.05, 0.005 and 0.0005 (significant). Non-significant correlations are indicated by the superscript **ns**. SWP or soil water potential used are the median values at 15 cm for each of these 5 sites (Von Arx et al., 2013). Water-extractable carbon is abbreviated to WEOC. Results indicate that no single climatic or textural factor consistently co-varies with carbon stocks, or turnover time.

Explaining variable	Stock <sub>0-20 cm</sub>	Turnover time bulk <sub>0-20 cm</sub>	Turnover time WEOC <sub>0-20 cm</sub>	Stock <sub>20-60 cm</sub>	Turnover time <sub>20-60 cm</sub>	Fraction dynamic <sub>0-20 cm</sub>
	cm	cm		cm		
MAT	0.17 <sup>ns</sup>	-0.12 <sup>ns</sup>	-0.36 <sup>ns</sup>	0.08 <sup>ns</sup>	0.04 <sup>ns</sup>	-0.15 <sup>ns</sup>
MAP	<b>0.96*</b>	0.04 <sup>ns</sup>	0.29 <sup>ns</sup>	<b>0.95*</b>	<b>0.97**</b>	<b>0.98*</b>
NPP	0.2 <sup>ns</sup>	0.68 <sup>ns</sup>	0.38 <sup>ns</sup>	0.07 <sup>ns</sup>	-0.05 <sup>ns</sup>	-0.36 <sup>ns</sup>
Sand	-0.66 <sup>ns</sup>	0.77 <sup>ns</sup>	0.53 <sup>ns</sup>	-0.58 <sup>ns</sup>	-0.65 <sup>ns</sup>	<b>-0.98*</b>
Silt	0.38 <sup>ns</sup>	<b>-0.94*</b>	-0.79 <sup>ns</sup>	0.29 <sup>ns</sup>	-0.40 <sup>ns</sup>	0.84 <sup>ns</sup>
Clay	<b>0.81*</b>	-0.57 <sup>ns</sup>	-0.29 <sup>ns</sup>	0.74 <sup>ns</sup>	0.79 <sup>ns</sup>	<b>0.99*</b>
CEC	-0.67 <sup>ns</sup>	-0.68 <sup>ns</sup>	-0.50 <sup>ns</sup>	<b>-0.98**</b>	<b>-0.98**</b>	0.16 <sup>ns</sup>
pH	-0.74 <sup>ns</sup>	-0.49 <sup>ns</sup>	-0.28 <sup>ns</sup>	-0.78 <sup>ns</sup>	-0.75 <sup>ns</sup>	0.20 <sup>ns</sup>
Fe	0.24 <sup>ns</sup>	-0.66 <sup>ns</sup>	-0.81 <sup>ns</sup>	-0.17 <sup>ns</sup>	-0.15 <sup>ns</sup>	-0.01 <sup>ns</sup>
Al	0.18 <sup>ns</sup>	-0.62 <sup>ns</sup>	-0.77 <sup>ns</sup>	-0.09 <sup>ns</sup>	-0.0 <sup>ns</sup>	-0.13 <sup>ns</sup>
SWP	0.70 <sup>ns</sup>	0.64 <sup>ns</sup>	0.71 <sup>ns</sup>	-	-	0.82 <sup>ns</sup>
Average		<b>0.95*</b>	<b>0.81*</b>	0.01 <sup>ns</sup>	-0.1 <sup>ns</sup>	-0.76 <sup>ns</sup>
Grain size	-0.25 <sup>ns</sup>					



Figures

**Figure 1** Sample locations, all of which are part of the Long-term ecosystem research program (LWF) of the Swiss Federal Institute WSL, 1) Othmarsingen, 2) Lausanne, 3) Aupal, 4) Beatenberg and 5) Nationalpark Image made using 2016 swisstopo (JD100042).

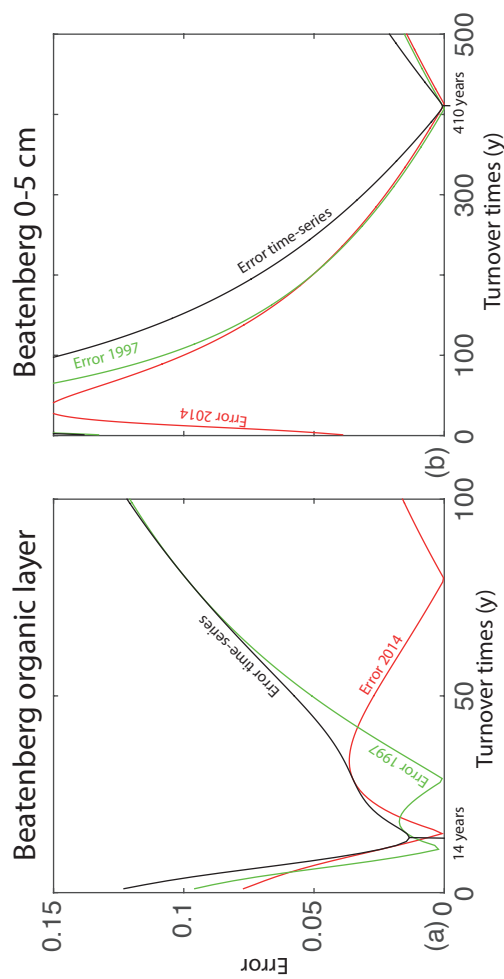


**Figure 2** Numerical optimization of least mean-square error reduction, showing and the reduction of error spread for two soil depths. For the Beatenberg organic layer (a) the individual time points yield two solutions are almost equally likely, but combined the time-points reveal the likeliest option. For the (b) 0-5 cm layer the single time points only have a single likely solution.

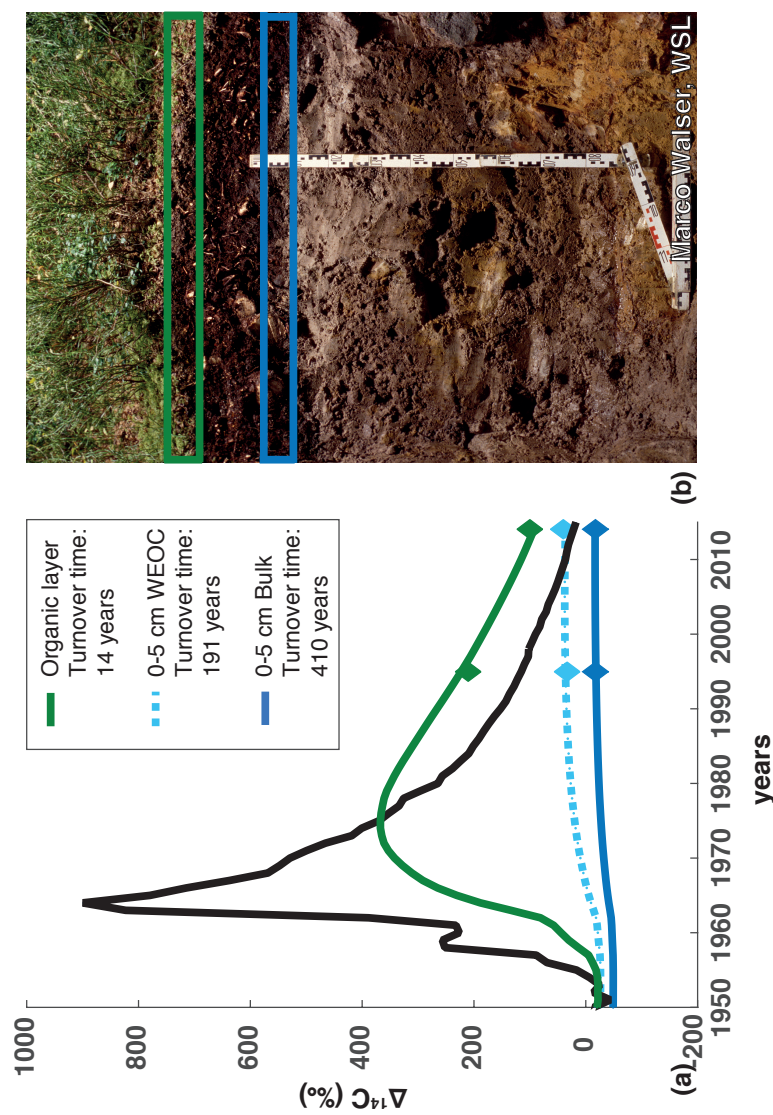


**Figure 3** (a) Time-series soil carbon turnover time in years (y) as determined by numerical modelling for (b) sub-alpine site Beatenberg. The bulk turnover in the organic layer is rapid (14 years), followed by the turnover of the water-extractable organic carbon (WEOC) (191 years) and the bulk turnover of the soil (410 years). Photo soil profile courtesy of Marco Walsler, WSL.

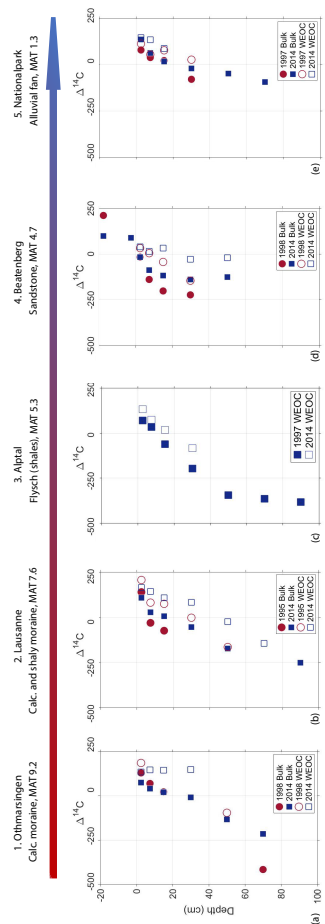


**Figure 4** (a-e) Changes in radiocarbon signature of both bulk soil and WEOC over two decades at four sites on a climatic gradient. For Alptal (c) only the 2014 time-point was available. For the warmer locations (Luvisol, Cambisol MAT 9.2-7.6 °C), depletion in bomb-derived radiocarbon occurs in the first five centimeters soil in 2014 as compared to 1995-8. The colder Beatenberg site (Podzol, MAT 4.7 °C) is marked by a clear enrichment of  $^{14}\text{C}$  in the mineral soil in 2014 w.r.t. 1997. At the coldest site Nationalpark (Fluvisol, MAT 1.3 °C) almost all samples taken two decades after the initial sampling show an enrichment in radiocarbon signature. WEOC contains bomb-derived carbon in the topsoil in 2014 at all sites.



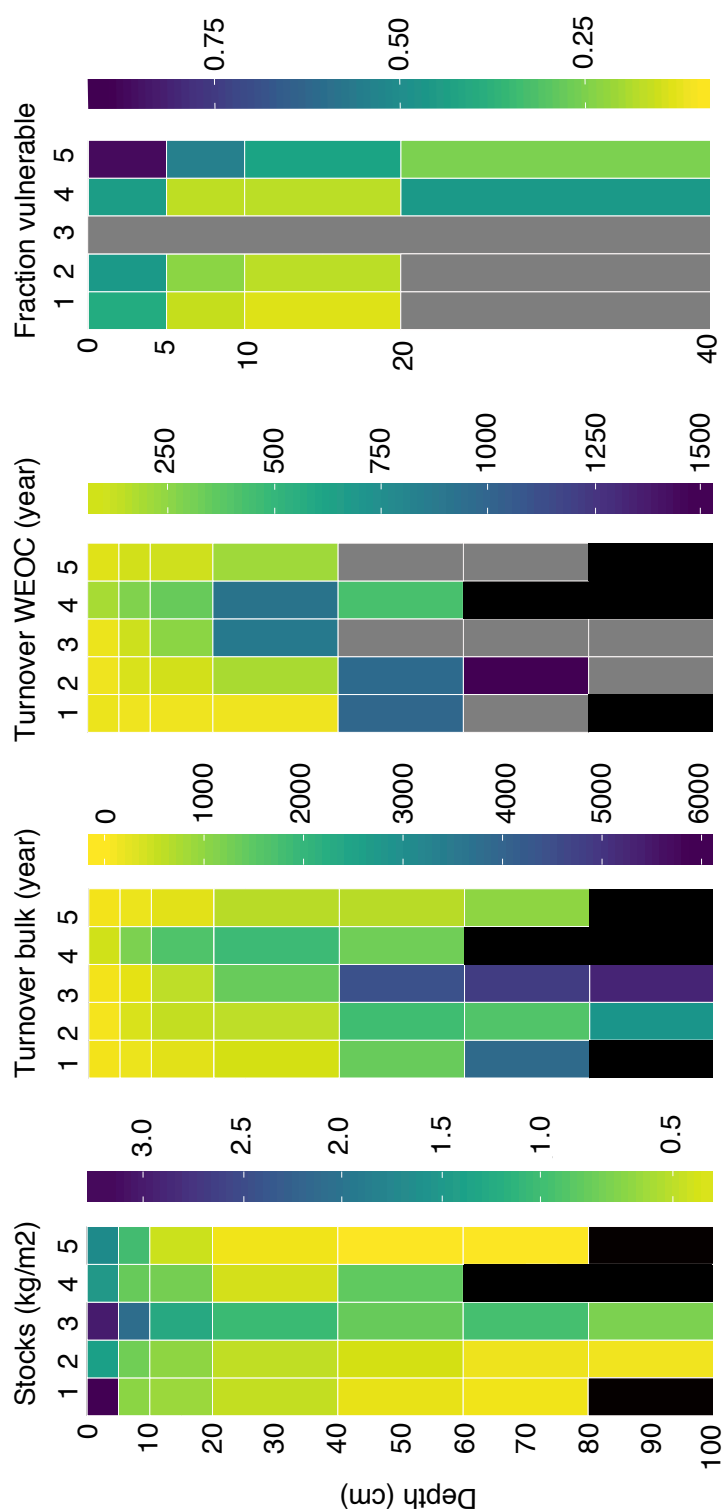


**Figure 5** Carbon (a) stocks in the mineral soil  $\text{kgC/m}^2$ , (b) turnover time bulk soil in years (c) turnover time water extractable organic carbon soil in years and (d) fraction vulnerable pool in 5 cm intervals. Locations are ordered from the warmest to coldest sites i.e. (1) Othmarsingen, (2) Lausanne, (3) Aiptal, (4) Beatenberg and (5) Nationalpark. Grey boxes indicate absence of material, black boxes indicate the occurrence of the C-horizon (poorly consolidated bedrock-derived stony material or bedrock itself).

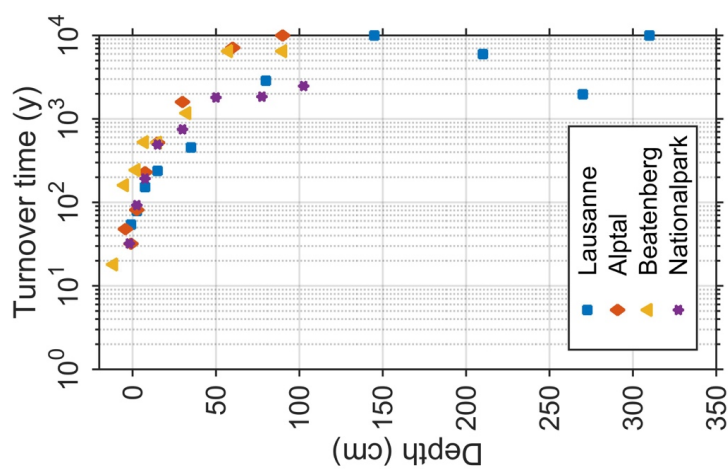


**Figure 6** Modeled turnover times (y) of single profiles sampled down to the bedrock between 1995 and 1998.  $\Delta^{14}\text{C}$  published in Van der Voort et al. (2016). Results indicate presence of petrogenic (bedrock-derived) carbon as modeled turnover time exceeds soil formation since the end of last ice age (10,000 years) in Lausanne (>100 cm, Cambisol) and Alptal (80-100 cm, Gleysol).